

# Phase Dynamics of Nearly Stationary Patterns in Activator-Inhibitor Systems

Aric Hagberg\*

Center for Nonlinear Studies and T-7, Theoretical Division,  
Los Alamos National Laboratory, Los Alamos, NM 87545

Ehud Meron†

The Jacob Blaustein Institute for Desert Research and the Physics Department,  
Ben-Gurion University, Sede Boker Campus 84990, Israel

Thierry Passot

Observatoire de la Côte d'Azur, BP 4229, 06304 Nice Cedex 4, France,  
and Department of Mathematics, University of Arizona, Tucson, AZ 85721

(Dated: December 2, 2024; Revised January 26, 2000)

The slow dynamics of nearly stationary patterns in a FitzHugh-Nagumo model are studied using a phase dynamics approach. A Cross-Newell phase equation describing slow and weak modulations of periodic stationary solutions is derived. The derivation applies to the bistable, excitable, and the Turing unstable regimes. In the bistable case stability thresholds are obtained for the Eckhaus and the zigzag instabilities and for the transition to traveling waves. Neutral stability curves demonstrate the destabilization of stationary planar patterns at low wavenumbers to zigzag and traveling modes. Numerical solutions of the model system support the theoretical findings.

## I. INTRODUCTION

Studies of stationary patterns in activator-inhibitor systems have focused primarily on localized structures such as pulses and spots in excitable and bistable media [1, 2, 3, 4, 5, 6, 7, 8], and periodic patterns near a Turing bifurcation [9, 10, 11]. Localized structures have instabilities to traveling patterns, breathing motion, and transverse deformations [2, 12, 13, 14]. Periodic patterns have been analyzed near the onset of a Turing instability and also near the codimension-two point of a Turing instability and a Hopf bifurcation [15, 16, 17, 18, 19]. But very few studies have explored instabilities of *periodic* (nonlocal) stationary patterns in excitable and bistable media, or of periodic stationary patterns *far beyond* the Turing instability [21, 22]. The latter case includes pattern formation studies on the CIMA chemical reaction [17, 23, 24].

In this paper we study instabilities of stationary periodic patterns by deriving a Cross-Newell phase equation [20, 25, 26]. The derivation is not restricted to the immediate neighborhood of a Turing instability and applies to periodic patterns with space-scale separation that arise far from onset or in excitable and bistable media. The Cross-Newell equation was originally derived in the context of fluid dynamics and has recently been applied in a laser system [27].

We choose to study the FitzHugh-Nagumo (FHN) equations, a canonical model for activator-inhibitor systems,

$$\begin{aligned} \frac{\partial u}{\partial t} &= u - u^3 - v + \nabla^2 u, \\ \frac{\partial v}{\partial t} &= \epsilon(u - a_1 v - a_0) + \delta \nabla^2 v. \end{aligned} \quad (1)$$

Here,  $u$  is the activator and  $v$  the inhibitor. The parameters  $a_0$  and  $a_1$  can be chosen so that the FHN model (1) represents

an excitable medium, a bistable medium, or a system with a Turing instability [13]. All three cases support stationary periodic solutions for  $\delta$  sufficiently large.

In Section II we derive a phase equation describing weak modulations of periodic stripe pattern in the FHN model. In Section III we evaluate stability thresholds for Eckhaus and zig-zag instabilities and for a transition from stationary to traveling patterns. These thresholds suggest a number of spatial or spatio-temporal behaviors which we test in Section IV with numerical solutions of Eqs. (1).

## II. THE PHASE EQUATION

Let  $u_0(\theta; k) = u_0(\theta + 2\pi; k)$ ,  $v_0(\theta; k) = v_0(\theta + 2\pi; k)$  be a stationary periodic solution of Eqs. (1) with phase  $\theta$  and wavenumber  $k$ . We consider weak spatial modulations of this periodic pattern and assume that those modulations have a length scale  $L$  that is much larger than the wavelength  $1/k$ . The ratio of the length scales  $\lambda = 1/(kL)$  can then be used as a small parameter to write modulated solutions as an asymptotic expansion about the periodic solution

$$\begin{aligned} u(\theta, \mathbf{R}, T) &= u_0(\theta; k) + \lambda u_1(\theta, \mathbf{R}, T) + \lambda^2 u_2(\theta, \mathbf{R}, T) + \dots \\ v(\theta, \mathbf{R}, T) &= v_0(\theta; k) + \lambda v_1(\theta, \mathbf{R}, T) + \lambda^2 v_2(\theta, \mathbf{R}, T) + \dots \end{aligned} \quad (2)$$

where  $\mathbf{R} = \lambda \mathbf{r}$  and  $T = \lambda^2 t$  are slow space and time variables. The phase  $\theta$  in Eq. (2) is an undetermined function of space and time and  $k = |\mathbf{k}| = |\nabla \theta|$  is the local wavenumber. Our objective is to derive an equation for the slow phase

$$\Theta(\mathbf{R}, T) := \lambda \theta(\mathbf{r}, \mathbf{R}, T).$$

In terms of this phase the local wavevector is

$$\mathbf{k}(\mathbf{R}, T) = \nabla_R \Theta .$$

Inserting the expansions (2) in Eqs. (1) we find at order unity

$$u_0 - u_0^3 - v_0 + k^2 \frac{\partial^2 u_0}{\partial \theta^2} = 0, \quad (3a)$$

$$\epsilon(u_0 - a_1 v_0 - a_0) + \delta k^2 \frac{\partial^2 v_0}{\partial \theta^2} = 0, \quad (3b)$$

where  $k^2 = \mathbf{k} \cdot \mathbf{k}$ . At order  $\lambda$

$$\left( k^2 \frac{\partial^2}{\partial \theta^2} + 1 - 3u_0^2 \right) u_1 - v_1 = \mathcal{D} \frac{\partial u_0}{\partial \theta}, \quad (4a)$$

$$\epsilon u_1 + \left( \delta k^2 \frac{\partial^2}{\partial \theta^2} - \epsilon a_1 \right) v_1 = \mathcal{D} \frac{\partial v_0}{\partial \theta}, \quad (4b)$$

where

$$\mathcal{D} = \frac{\partial \Theta}{\partial T} - \nabla_R \cdot \mathbf{k} - 2\mathbf{k} \cdot \nabla_R. \quad (5)$$

Projecting the right hand side of (4) onto  $(\partial_\theta u_0, -\epsilon^{-1} \partial_\theta v_0)$ , the solution of the adjoint problem, produces the phase equation

$$\tau \frac{\partial \Theta}{\partial T} = -\nabla_R \cdot (\mathbf{k}B),$$

where

$$\begin{aligned} \tau &= <(\partial_\theta u_0)^2> - \epsilon^{-1} <(\partial_\theta v_0)^2>, \\ B &= - <(\partial_\theta u_0)^2> + \delta \epsilon^{-1} <(\partial_\theta v_0)^2>. \end{aligned} \quad (6)$$

In these equations  $<(\cdot)> := \frac{1}{2\pi} \int_0^{2\pi} (\cdot) d\theta$ .

The quantities  $B$  and  $\tau$  contain information about various instabilities of the periodic stripe pattern. The condition  $\frac{d}{dk} [kB(k)] = 0$  implies the onset of an Eckhaus instability and the condition  $B = 0$  the onset of a zigzag instability [25]. In Appendix A we show that the condition  $\tau = 0$  indicates a transition to traveling waves.

To implement these conditions we need to solve Eqs. (3) for the periodic solution  $(u_0, v_0)$ . For parameter values that satisfy  $\epsilon/\delta := \mu \ll 1$  an approximate solution can be computed as shown in Appendix B. Using this solution to calculate  $\tau$  and  $B$ , as shown in Appendix C, gives the following expressions:

$$\begin{aligned} \tau &= \frac{2\sqrt{2}}{3\pi k} - \frac{v_-}{q\pi k\eta} \beta(\Lambda_-) \gamma(\Lambda_-, \Lambda_+), \\ B &= \frac{2\sqrt{2}}{3\pi k} - \frac{v_-}{q\pi k\sqrt{\mu}} \beta(\Lambda_-) \gamma(\Lambda_-, \Lambda_+), \end{aligned} \quad (8)$$

$$\Lambda_- + \Lambda_+ = \frac{2\pi\sqrt{\mu}}{k}, \quad (9)$$

$$v_+ \beta(\Lambda_+) + v_- \beta(\Lambda_-) = 0, \quad (10)$$

where  $\mu = \epsilon/\delta$ ,  $\eta = \sqrt{\epsilon\delta}$ ,  $v_\pm = (\pm 1 - a_0)/q^2$ ,  $q^2 = a_1 + 1/2$ ,

$$\beta(x) = \coth qx - \operatorname{csch} qx, \quad (11)$$

and

$$\begin{aligned} \gamma(\Lambda_-, \Lambda_+) &= -1 + \frac{1}{2}(1 + a_0)q\Lambda_- \operatorname{csch} q\Lambda_- \\ &\quad + \frac{1}{2}(1 - a_0)q\Lambda_+ \operatorname{csch} q\Lambda_+. \end{aligned} \quad (12)$$

The quantities  $\Lambda_+$  and  $\Lambda_-$  denote the widths of domains with high and low values of  $u$  and  $v$ , respectively. The width is measured with respect to the spatial coordinate  $z = \frac{\sqrt{\mu}}{k}\theta$  (see Appendix B). Given  $k$ , Eqs. (9) and (10) can be solved for  $\Lambda_+(k)$  and  $\Lambda_-(k)$ . Using these solutions in Eq. (8) graphs of  $\tau$  and  $kB$  as functions of  $k$  can be produced.

### III. STABILITY THRESHOLDS

Explicit forms for  $\tau(k)$  and  $B(k)$  are available in the symmetric case,  $a_0 = 0$ , where  $\Lambda_+ = \Lambda_- = \frac{\pi\sqrt{\mu}}{k}$ :

$$\begin{aligned} \tau(k) &= \frac{1}{\pi k \eta_c q^3} \left[ 1 - \frac{\eta_c}{\eta} f(\pi q \sqrt{\mu}/k) \right], \\ B(k) &= \frac{1}{\pi k \eta_c q^3} \left[ 1 - \frac{\eta_c}{\sqrt{\mu}} f(\pi q \sqrt{\mu}/k) \right], \end{aligned} \quad (13)$$

where  $\eta_c = \frac{3}{2\sqrt{2}q^3}$  and

$$f(x) = (1 - x \operatorname{csch} x)(\coth x - \operatorname{csch} x). \quad (14)$$

Figure 1 shows graphs of  $\tau(k)$  and  $kB(k)$  for a bistable medium obtained with Eqs. (13) (thick lines) and with Eqs. (6) and (7) using numerically calculated solutions  $u_0, v_0$  (circles). A very good agreement is obtained within the validity range of the analysis,  $k \sim \mathcal{O}(\sqrt{\mu}) \ll 1$ . For  $k \sim \mathcal{O}(1)$  the deviations become large. In particular the minimum of  $kB(k)$  which designates the Eckhaus instability threshold, is not reproduced by the analytical form (13).

The instability to traveling waves occurs at  $\tau = 0$  or at

$$\epsilon = \eta_c^2 f^2(\pi q \sqrt{\mu}/k) \delta^{-1}. \quad (15)$$

The zigzag instability occurs at  $B = 0$  or at

$$\epsilon = \eta_c^2 f^2(\pi q \sqrt{\mu}/k) \delta. \quad (16)$$

The condition  $\frac{d}{dk}(kB) = 0$  for the Eckhaus instability becomes

$$\frac{df}{dx}|_{x=\pi q \sqrt{\mu}/k} = 0.$$

Consider first the limit  $k \rightarrow 0$  in which the periodic pattern approaches an array of isolated front structures. In this limit  $f(\pi q \sqrt{\mu}/k) \rightarrow 1$  and the condition for the onset of traveling waves becomes  $\epsilon = \eta_c^2 \delta^{-1}$ . This is precisely the nonequilibrium Ising-Bloch (NIB) bifurcation point, where a stationary

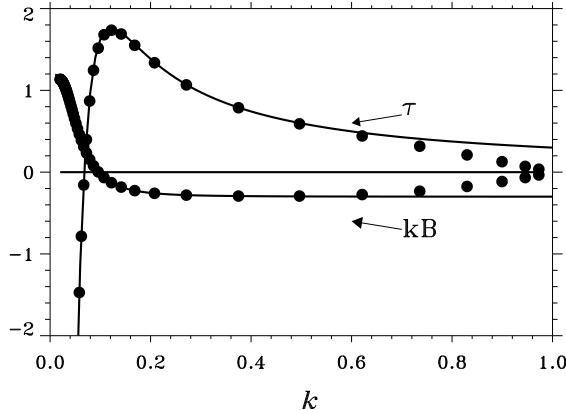


FIG. 1: Typical functions  $\tau(k)$  and  $kB(k)$  for a bistable medium. The curves represent the functions of Eqs. (13). The circles are numerically computed solutions using Eqs. (6) and (7). The point  $kB = 0$  indicates the boundary between stable stationary stripes and zigzag patterns. At  $\tau = 0$  the pattern becomes unstable to traveling waves. Parameters:  $a_1 = 4$ ,  $a_0 = 0$ ,  $\epsilon = 0.001$ ,  $\delta = 2.0$ .

front loses stability to a pair of counter-propagating fronts. The condition for the zigzag instability becomes  $\epsilon = \eta_c^2 \delta$ . This is the threshold for the transverse front instability [28].

The neutral stability curves for a bistable medium corresponding to Eqs. (15) and (16) are shown in Figs. 2a and 2b for fixed  $\delta$  and  $\epsilon$ , respectively. They imply that high wavenumber stationary planar patterns are stabilized against zigzag and traveling wave instabilities. Notice that for  $\delta = 1$  the neutral stability curves  $\tau = 0$  and  $B = 0$  coincide (see Eqs. (15) and (16) or Fig. 2b). For  $\delta > 1$ , upon decreasing the wavenumber at constant  $\epsilon$ , a high wavenumber pattern is destabilized to a zigzag pattern, whereas for  $\delta < 1$  the destabilization is to traveling waves. Similar neutral stability curves are found for the nonsymmetric case,  $a_0 \neq 0$ , for excitable media and for systems (far) beyond the Turing instability.

#### IV. COMPARISONS WITH NUMERICAL SOLUTIONS

We have computed numerical solutions of Eqs. (1) to test the stabilization of zigzag and traveling-wave instabilities at high wavenumbers. Figure 3 shows a low wavenumber zigzag pattern and a high wavenumber planar pattern computed for the same parameter values. This behavior is well known in other contexts [29]. The zigzag instability is a mechanism by which the system locally increases the wavenumber. Figure 4 shows coexistence of a low wavenumber traveling wave and a high wavenumber stationary pattern. These numerical results are for a bistable system but similar results are found for excitable and Turing unstable systems. Coexistence of stationary and traveling waves has been found in experiments on the CIMA reaction [17, 24], and analyzed using different theoretical approaches [21, 22, 30, 31].

We have also tested the condition for the Eckhaus instability in a bistable system using numerical computations of  $\tau$

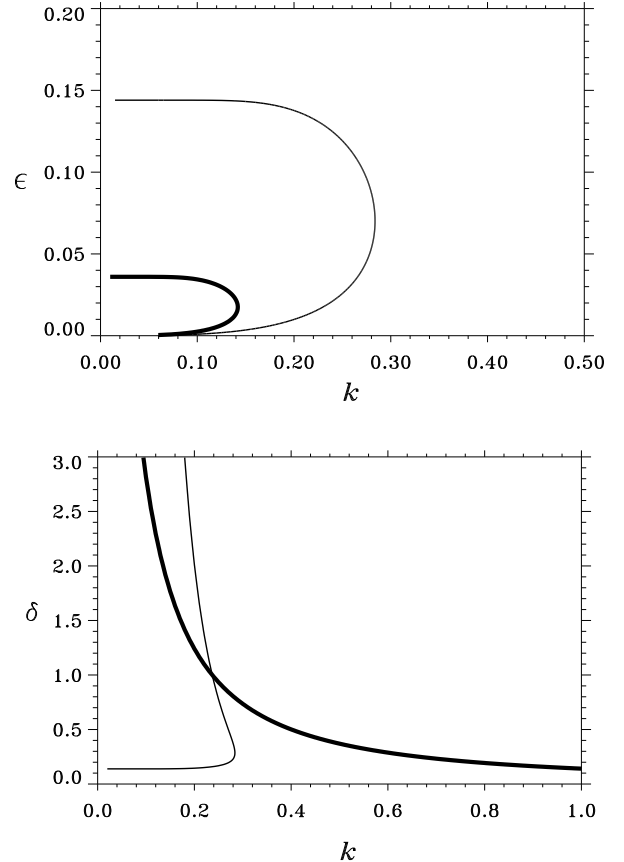


FIG. 2: The neutral stability boundaries for the zigzag instability ( $B = 0$ ; thick, solid curve) and traveling wave instability ( $\tau = 0$ ; thin, dashed curve). To the left of the  $B = 0$  curve planar periodic patterns are unstable to zigzag patterns. To the left of the  $\tau = 0$  curve planar periodic patterns are unstable to traveling waves. Parameters:  $a_1 = 2$ ,  $a_0 = 0$ ,  $\epsilon = 0.01$ ,  $\delta = 2$ .

and  $B$ . Choosing wavenumbers  $k > k_c$  where  $k_c$  corresponds to the minimum of  $kB$ , we found initial periodic patterns either collapse to uniform states or to a lower wavenumber pattern through phase slips. Fig. 5 demonstrates these two cases. Similar conclusions hold for excitable systems. An unstable Turing pattern, on the other hand, always converges to a lower wavenumber pattern since the single uniform state is unstable.

#### V. CONCLUSION

We have shown that the Cross-Newell phase equation provides a powerful tool for studying instabilities of stationary periodic patterns in activator-inhibitor systems. The equation contains information not only on the Eckhaus and zigzag instabilities, but also on the destabilization of stationary periodic patterns to traveling waves. The same equation applies to bistable, excitable, and Turing unstable systems. Equations of that kind should prove useful in identifying parameters and

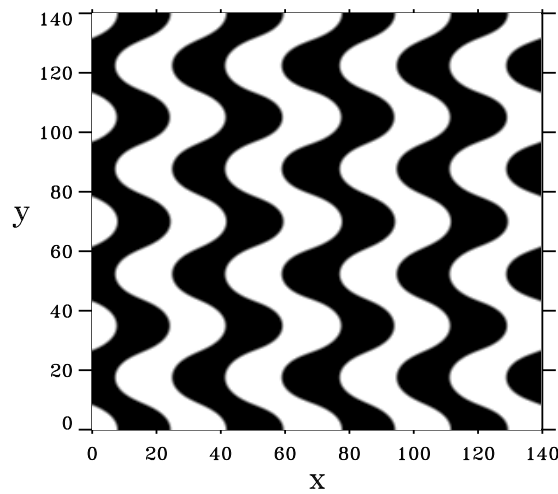
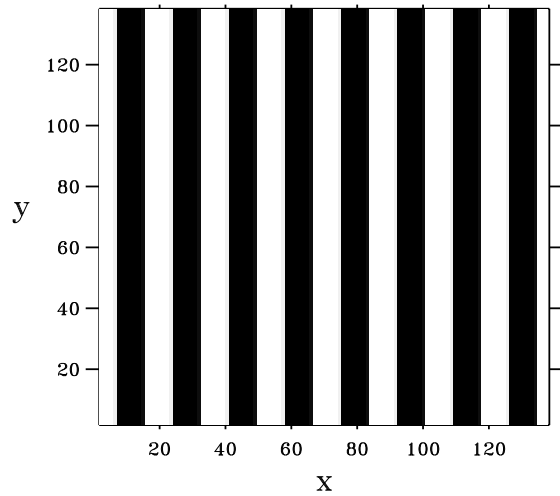


FIG. 3: Coexistence of zigzag and planar patterns. The dark areas indicate regions of  $u > 0$  and the light regions  $u < 0$ . At higher wavenumbers (top) the planar stripe solution is stable. At low wavenumbers (bottom) the planar solution is unstable and forms a zigzag pattern. Parameters:  $a_1 = 2$ ,  $a_0 = 0$ ,  $\epsilon = 0.05$ ,  $\delta = 2$ .

initial conditions where zigzag and Eckhaus instabilities couple to traveling wave modes. Such coupling may lead to complex spatiotemporal behavior analogous to the coupling of the NIB front bifurcation to a transverse front instability [28, 32]

### Acknowledgments

This study was supported in part by grant No 95-00112 from the US-Israel Binational Science Foundation (BSF) and by the Department of Energy, under contract W-7405-ENG-36.

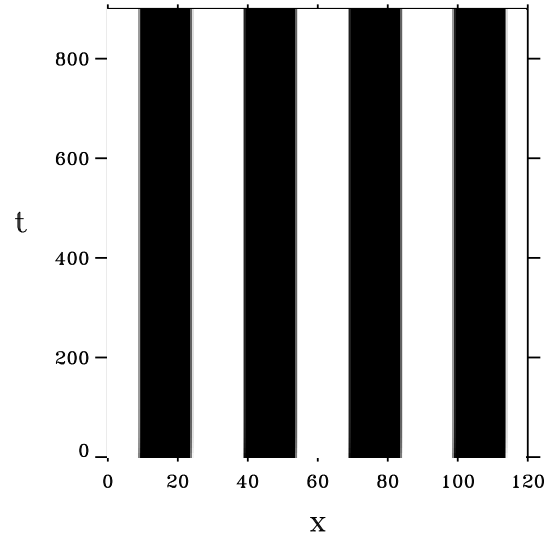


FIG. 4: Coexistence of traveling waves and stationary waves. At high wavenumber (top) the patterns are stationary and at low wavenumber patterns (bottom) they travel. Parameters:  $a_1 = 2$ ,  $a_0 = 0$ ,  $\epsilon = 0.03$ ,  $\delta = 2$ .

### APPENDIX A: THE MEANING OF $\tau = 0$

We show here that the condition  $\tau = 0$  defines the critical value of  $\epsilon$  at which traveling solutions bifurcate from the stationary solution. We look for traveling solutions  $u(\theta), v(\theta)$  of Eqs. (1), where  $\theta = kx - \omega t$ , that bifurcate from the stationary solution branch  $\omega = 0$  at some  $\epsilon = \epsilon_c$ . Near the bifurcation where  $\omega \ll 1$  we can expand the traveling solutions as power series in  $\omega$  around the stationary solution  $u_0, v_0$ :

$$\begin{aligned} u(\theta) &= u_0(\theta) + \omega u_1(\theta) + \dots, \\ v(\theta) &= v_0(\theta) + \omega v_1(\theta) + \dots, \end{aligned} \quad (\text{A1})$$

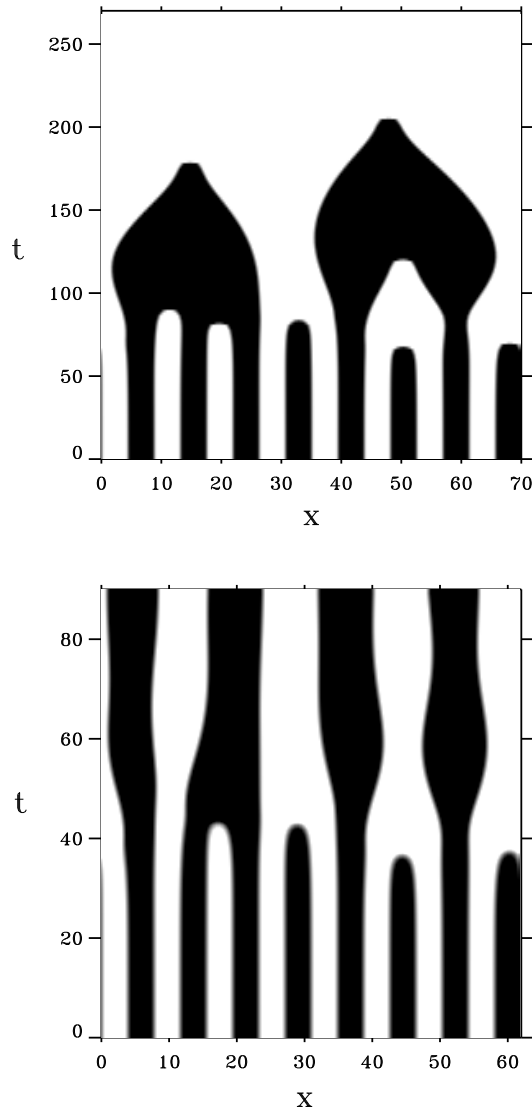


FIG. 5: Time evolution of a periodic pattern in the region of Eckhaus instability. The high wavenumber pattern is unstable and either converges to one of the uniform states (top) or a lower wavenumber pattern (bottom). Parameters:  $a_1 = 2, a_0 = 0, \delta = 2$ ; top:  $\epsilon = 0.01$ , bottom:  $\epsilon = 0.1$ .

Expanding  $\epsilon$  as

$$\epsilon = \epsilon_c + \epsilon_1 \omega + \dots, \quad (\text{A2})$$

and using these expansions in Eqs. (1) we find at order  $\omega$

$$\begin{aligned} \left( k^2 \frac{\partial^2}{\partial \theta^2} + 1 - 3u_0^2 \right) u_1 - v_1 &= -u_0', \\ \epsilon_c u_1 + \left( \delta k^2 \frac{\partial^2}{\partial \theta^2} - \epsilon a_1 \right) v_1 &= -v_0' - \epsilon_1 (u_0 - a_1 v_0 - a_0). \end{aligned}$$

Projecting the right hand side onto  $(u_0', -\epsilon_c^{-1} v_0')$  gives

$$\epsilon_c = \frac{\langle u_0'^2 \rangle}{\langle u_0'^2 \rangle}, \quad (\text{A3})$$

where we used Eq. (3b) and switched to the notation of a prime for the derivative with respect to the single argument  $\theta$ . Using the definition (6) of  $\tau$  and (A3) we find

$$\tau = \left( 1 - \frac{\epsilon_c}{\epsilon} \right) \langle u_0'^2 \rangle. \quad (\text{A4})$$

Thus,  $\tau = 0$  implies  $\epsilon = \epsilon_c$  or the onset of traveling solutions.

## APPENDIX B: APPROXIMATE STATIONARY SOLUTION

For  $\mu = \epsilon/\delta \ll 1$  a singular perturbation approach can be used to approximate the stationary solution  $u_0(\theta), v_0(\theta)$ . Rescaling the space coordinate as  $z = \frac{\sqrt{\mu}}{k}\theta$ , Eqs. (3) become

$$\begin{aligned} u_0 - u_0^3 - v_0 + \mu u_0'' &= 0, \\ u_0 - a_1 v_0 - a_0 + v_0'' &= 0, \end{aligned}$$

where the prime denotes now the derivative with respect to  $z$ . Since the small parameter  $\mu$  multiplies the second derivative term  $u_0''$ , two types of spatial regions can be distinguished. Outer regions where  $u_0(z)$  varies on a scale of order unity and the term  $\mu u_0''$  is negligible, and inner regions where  $u_0(z)$  varies on a very short scale of order  $\sqrt{\mu}$  and the term  $\mu u_0''$  cannot be neglected. In these regions, however,  $v_0$  hardly changes.

The analysis of the inner regions leads to the solutions

$$u_0 = \pm \tanh \frac{\theta}{\sqrt{2k}}, \quad v_0 = 0. \quad (\text{B1})$$

These solution represent front structures separating two types of outer regions: domains of high activator values,  $u = u_+(v_0)$  ("up state"), and domains of low activator values  $u = u_-(v_0)$  ("down state"), where  $u_{\pm}(v_0)$  are the extreme roots of  $u_0 - u_0^3 - v_0 = 0$ . We look for periodic stationary solutions with wavelength  $\Lambda = \Lambda_- + \Lambda_+$ , where  $\Lambda_+$  and  $\Lambda_-$  are the widths of up and down states respectively. Consider now a down state spanning the spatial range  $-\Lambda_- < z < 0$  followed by an up state spanning the range  $0 < z < \Lambda_+$ . The equations for  $v$  at these outer regions are

$$v_0'' - q^2(v_0 - v_-) = 0, \quad -\Lambda_- < z < 0, \quad (\text{B2})$$

with the boundary conditions  $v_0(-\Lambda_-) = v_0(0) = 0$ , and

$$v_0'' - q^2(v_0 - v_+) = 0, \quad 0 < z < \Lambda_+, \quad (\text{B3})$$

with the boundary conditions  $v_0(0) = v_0(\Lambda_+) = 0$ . In obtaining these equations we approximated  $u_{\pm}(v_0) = \pm 1 - v_0/2$ . This approximation is particularly good for bistable media with  $a_0$  small and  $a_1$  relatively large. These values restrict  $v_0$  to a small range around  $v_0 = 0$ . For excitable media and

systems undergoing Turing instability, a large value of  $\delta$  might be needed to keep  $v_0$  small.

The solutions to Eqs. (B2) and (B3) are

$$v_0 = \frac{v_-}{\sinh q\Lambda_-} [\sinh qz - \sinh q(z + \Lambda_-)] + v_-, \quad (\text{B4})$$

for  $-\Lambda_- < z < 0$ , and

$$v_0 = \frac{v_+}{\sinh q\Lambda_+} [\sinh q(z - \Lambda_+) - \sinh qz] + v_+, \quad (\text{B5})$$

for  $0 < z < \Lambda_+$ . To determine  $\Lambda_\pm$  for a given  $\Lambda$  we match the derivatives of  $v_0$  at the front positions

$$v'_0(0^+) = v'_0(0^-), \quad v'_0(\Lambda_+) = v'_0(-\Lambda_-).$$

This leads to the relation

$$v_+ \beta(q\Lambda_+) + v_- \beta(q\Lambda_-) = 0,$$

where  $\beta(x)$  is given by Eq. (11).

### APPENDIX C: CALCULATION OF $\tau$ AND $B$

The quantities  $\tau$  and  $B$  are given by Eqs. (6) and (7). Consider first the integral

$$\langle u'_0(\theta)^2 \rangle = \frac{1}{2\pi} \int_0^{2\pi} u'_0(\theta)^2 d\theta.$$

It has a contribution from two inner regions at  $z = 0$  and  $z = \Lambda_+$  where  $u_0$  is given by Eq. (B1), and a contribution from two outer regions,  $-\Lambda_- < z < 0$  and  $0 < z < \Lambda_+$  where  $u_0 = -1 - v_0/2$  and  $u_0 = 1 - v_0/2$  with  $v_0$  given by Eq. (B4) and Eq. (B5), respectively. (Recall that  $z = \frac{\sqrt{\mu}}{k}\theta$ ).

The contribution from the two inner regions is

$$\begin{aligned} \langle u'_0(\theta)^2 \rangle_{inner} &= \frac{1}{2\pi k^2} \int_{inner} \operatorname{sech}^4 \left( \frac{\theta}{\sqrt{2}k} \right) d\theta, \\ &\approx \frac{1}{\sqrt{2}\pi k} \int_{-\infty}^{\infty} \operatorname{sech}^4 x dx = \frac{2\sqrt{2}}{3\pi k}. \end{aligned}$$

We have used here the fact that  $k \sim \mathcal{O}(\sqrt{\mu}) \ll 1$ . The integral over a narrow inner region is transformed into an integral over a wide region after stretching the  $\theta$  variable to the  $x = \frac{\theta}{\sqrt{2}k}$  variable. The contribution from the two outer regions is

$$\begin{aligned} \langle u'_0(\theta)^2 \rangle_{outer} &= \frac{\sqrt{\mu}}{8\pi k} \\ &\times \left[ \int_{-\Lambda_-}^0 v_0(z)^{\prime 2} dz + \int_0^{\Lambda_+} v_0(z)^{\prime 2} dz \right], \end{aligned}$$

where we used in the two outer regions  $u_0(z)' = -\frac{1}{2}v_0(z)'$ . Altogether,

$$\begin{aligned} \langle u'_0(\theta)^2 \rangle &= \frac{2\sqrt{2}}{3\pi k} + \frac{\sqrt{\mu}}{8\pi k} \\ &\times \left[ \int_{-\Lambda_-}^0 v_0(z)^{\prime 2} dz + \int_0^{\Lambda_+} v_0(z)^{\prime 2} dz \right]. \end{aligned} \quad (\text{C1})$$

The second term on the right hand side of Eq. (C1) is small (since  $\sqrt{\mu} \ll 1$ ) and will not contribute to the leading order forms of  $\tau$  and  $B$ .

Consider now the integral

$$\langle v'_0(\theta)^2 \rangle = \frac{1}{2\pi} \int_0^{2\pi} v'_0(\theta)^2 d\theta.$$

The contribution from the inner regions to this integral is negligible for  $\mu \ll 1$ . Thus

$$\begin{aligned} \langle v'_0(\theta)^2 \rangle &= \frac{\sqrt{\mu}}{2\pi k} \\ &\times \left[ \int_{-\Lambda_-}^0 v_0(z)^{\prime 2} dz + \int_0^{\Lambda_+} v_0(z)^{\prime 2} dz \right]. \end{aligned} \quad (\text{C2})$$

Using the solutions (B4) and (B5) in the integrals (C1) and (C2) and using the expressions for  $\tau$  and  $B$  we obtain the expressions (8).

\* Electronic address: aric@lanl.gov

† Electronic address: ehud@bgu-mail.bgu.ac.il

- [1] J. J. Tyson and J. P. Keener, *Physica D* **32**, 327 (1988).
- [2] B. S. Kerner and V. V. Osipov, *Sov. Phys. Usp.* **32**(2), 101 (1989), *usp. Fiz. Nauk* **157** 201-266 (February 1989).
- [3] E. Meron, *Phys. Rep.* **218**(1), 1 (1992).
- [4] K. Krischer and A. Mikhailov, *Phys. Rev. Lett.* **73**, 3165 (1994).
- [5] K. J. Lee and H. L. Swinney, *Phys. Rev. E* **51**(3), 1899 (1995).
- [6] C. B. Muratov and V. V. Osipov, *Phys. Rev. E* **53**(4), 3101 (1996).
- [7] R. Woesler, P. Schütz, M. Bode, M. Or-Guil, and H.-G. Purwins, *Physica D* **91**, 376 (1996).
- [8] C. P. Schenk, M. Or-Guil, M. Bode, and H. G. Purwins, *Phys. Rev. Lett.* **78**, 3781 (1997).
- [9] V. Castets, D. Dulos, J. Boissonade, and P. D. Kepper, *Phys. Rev. Lett.* **64**, 2953 (1990).
- [10] Q. Ouyang and H. L. Swinney, *Nature* **352**, 610 (1991).
- [11] E. Ammelt, Y. A. Astrov, and H. G. Purwins, *Phys. Rev. E* **55**, 6731 (1997).
- [12] T. Ohta, M. Mimura, and R. Kobayashi, *Physica D* **34**, 115 (1989).
- [13] A. Hagberg and E. Meron, *Nonlinearity* **7**, 805 (1994), URL <http://math.lanl.gov/People/aric/Papers/frontbif/>.
- [14] R. E. Goldstein, D. J. Muraki, and D. M. Petrich, *Phys. Rev. E* **53**(4), 3933 (1996).
- [15] A. Rovinsky and M. Menzinger, *Phys. Rev. A* **46**, 6315 (1992).
- [16] A. G. Heidemann, M. Bode, and H. G. Purwins, *Phys. Lett. A*

**177**, 225 (1993).

[17] J. J. Peraud, A. D. Wit, E. Dulos, P. D. Kepper, G. Dewel, and P. Borckmans, *Phys. Rev. Lett.* **71**, 1272 (1993).

[18] A. D. Wit, D. Lima, G. Dewel, and P. Borckmans, *Phys. Rev. E* **54**, 261 (1996).

[19] M. Or-Guil and M. Bode, *Physica A* **249**, 174 (1998).

[20] L. Kramer, E. Ben Jacob, H. Brand, and M. C. Cross, *Phys. Rev. Lett.* **49**, 1891 (1982).

[21] J. D. Dockery and J. P. Keener, *SIAM J. Appl. Math.* **49**, 539 (1989).

[22] V. V. Osipov, *Physica D* **93**, 143 (1996).

[23] Q. Ouyang and H. L. Swinney, *Chaos* **1**, 411 (91).

[24] P. D. Kepper, J. J. Peraud, B. Rudovics, and E. Dulos, *Int. J. Bif. Chaos* **4**(5), 1215 (1994).

[25] M. C. Cross and A. C. Newell, *Physica D* **10**, 199 (1984).

[26] A. C. Newell, T. Passot, C. Bowman, N. Ercolani, and R. Indik, *Physica D* **97**, 185 (1996).

[27] J. Lega, J. V. Moloney, and A. C. Newell, *Physica D* **83**, 478 (1995).

[28] A. Hagberg and E. Meron, *Chaos* **4**(3), 477 (1994), URL <http://math.lanl.gov/People/aric/Papers/complex/>.

[29] M. C. Cross and P. C. Hohenberg, *Rev. Mod. Phys.* **65**(3), 851 (1993).

[30] A. Ito and T. Ohta, *Phys. Rev. A* **45**, 8374 (1992).

[31] E. M. Kuznetsova and V. V. Osipov, *Phys. Rev. E* **51**, 148 (1995).

[32] A. Hagberg and E. Meron, *Phys. Rev. Lett.* **72**(15), 2494 (1994), URL <http://math.lanl.gov/People/aric/Papers/turb/>.